
MOTIONAL REPRESENTATION; THE ABILITY TO PREDICT ODOR CHARACTERS USING MOLECULAR VIBRATIONS

A PREPRINT

 **Yuki Harada**

Research and Education Institute for Semiconductors and Informatics Laboratory for Data Sciences of Kumamoto University, Kurokami 2-39-1, Chuo-ku, Kumamoto 860-8555, JP
yharada@kumamoto-u.ac.jp

 **Shuichi Maeda**

Research and Education Institute for Semiconductors and Informatics Laboratory for Data Sciences of Kumamoto University, Kurokami 2-39-1, Chuo-ku, Kumamoto 860-8555, JP
Shuichi2503736@gmail.com

 **Junwei Shen**

Research and Education Institute for Semiconductors and Informatics Laboratory for Data Sciences of Kumamoto University, Kurokami 2-39-1, Chuo-ku, Kumamoto 860-8555, JP
jwshen@kumamoto-u.ac.jp

 **Taku Misonou**

University of Yamanashi, Emeritus Professors, Takeda 4-4-37
Kofu, Yamanashi, 400-8510, JP
tmisonou@gmail.com

 **Hirokazu Hori**

University of Yamanashi, Emeritus Professors, Takeda 4-4-37
Kofu, Yamanashi, 400-8510, JP
hirohori@yamanashi.ac.jp

 **Shinichiro Nakamura**

Research and Education Institute for Semiconductors and Informatics Laboratory for Data Sciences of Kumamoto University, Kurokami 2-39-1, Chuo-ku, Kumamoto 860-8555, JP
shindon@kumamoto-u.ac.jp

September 23, 2025

ABSTRACT

The prediction of odor characters is still impossible based on the odorant molecular structure. We designed a CNN-based regressor for computed parameters in molecular vibrations (CNN_vib), in order to investigate the ability to predict odor characters of molecular vibrations. In this study, we explored following three approaches for the predictability; (i) CNN with molecular vibrational parameters, (ii) logistic regression based on vibrational spectra, and (iii) logistic regression with molecular fingerprint(FP). Our investigation demonstrates that both (i) and (ii) provide predictability, and also that the vibrations as an explanatory variable (i and ii) and logistic regression with fingerprints (iii) show nearly identical tendencies. The predictabilities of (i) and (ii), depending on odor descriptors, are comparable to those of (iii). Our research shows that odor is predictable by odorant molecular

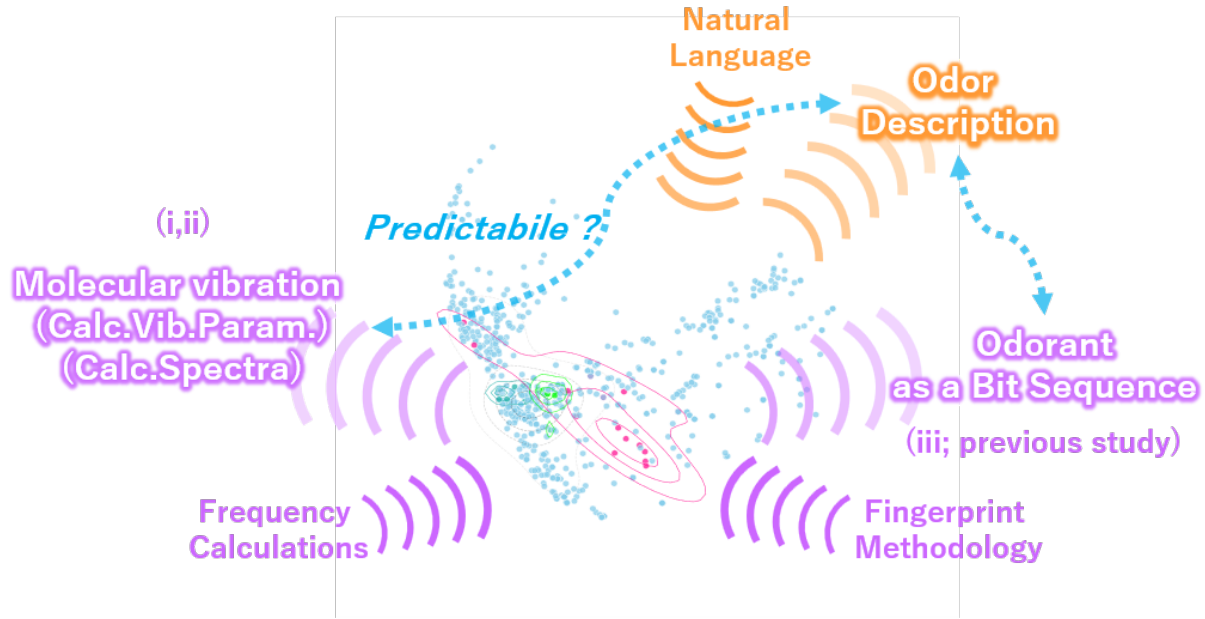


Figure 1: Comparison of three regressors to investigate the explanatory ability of molecular vibrations

vibration as well as their shapes alone. Our findings provide insight into the representation of molecular motional features beyond molecular structures.

Keywords odor · odorant · odor-sensing space · chemical space · molecular vibrations

1 Introduction

Odorants chemical space is the collection of volatilized chemical compounds that humans and many animals can perceive via their sense of smell. The total number of whole *chemical space* is estimated to be 10^{60} that is the collection of all potentially possible existing compounds, including those yet to be found. [1, 2] There could be almost 400,000 types of odor molecules in the odorant chemical space, in addition to the 20,000 known ones. [3, 4, 5] The prediction of perceived odor character / quality of odorants is an extremely challenging task based on their molecular structure. Because some odor character is not simply related directly to molecular structure, while others are related to molecular structure, such as aliphatic, aromatic, saturated, unsaturated, and polar.

There are different ways to represent chemical space, and there is no established implementation. [6, 7] Molecular fingerprint(FP) design is currently being refined, and there may be further approaches to detect molecular structure. [8] However machine learning with FP is a fundamental and/or irreplaceable approach for structure-activity relationship((Q)SAR) [9, 10] and quantitative structure-odor relationship (QSOR). [11] In our previous study, we reported the relation between the odor descriptors and their structural diversity for odorants groups associated with each odor descriptor. Using the logistic regression with conventional FPs, we investigated the influence of structural diversity on the odor descriptor predictability. [12]

Since Richard Axel and Linda Buck discovered the role of G-protein-coupled receptors in olfactory cells in the 1990s, the biological mechanisms in the olfactory system have been successfully and thoroughly elucidated up to the present day. The primary stage of olfaction is the chemical interactions between olfactory receptors (around 400 types) and odorants (odor molecules, more than 20,000 types). [3, 4, 5] The *shape theory of olfaction*, meaning that odorant molecules are recognized by their shapes, is no doubt. The *vibrational theory of olfaction*, which was a complementary previous hypothesis to it, means that odorant molecular vibrations are responsible for olfaction rather than their shapes alone. While the *shape theory of olfaction* is widely accepted concept of the olfaction, some researchers feel that both the form and vibrational properties of molecules have a role in olfaction. [13, 14, 15]

In this study, we investigated whether the molecular vibration is effective and whether the current representation is sufficient for the molecular feature, as shown in Fig.1. We compared predictability of three regressors; (i) CNN_vib with vibrational parameters, (ii) logistic regression based on vibrational spectra, and (iii) logistic regression with

conventional FPs. For (i), we designed a CNN-based regressor with the quantum chemically computed parameters, we call it 'CNN_vib' in this paper. For (iii), we already reported a study. [12] As a natural extention of previous study, we evaluated differences in predictabilities of each regression from (i) and (ii). We will conclude and discuss the possibility of molecular vibration in odorants chemicals. Finally, we discuss focusing on the motional representation using molecular vibration beyond substructures.

2 Materials and methods

2.1 Odorants and odor descriptors in the flavornet database

The data is collected from articles published since 1984 using GCO to detect odorants in natural products. It is available in pyrfume database [5] as well as Flavornet online database. [16] It is a compilation of aroma compounds found in the human odor space. The odorants are arranged by chromatographic and odor descriptors.

2.2 Vibrational frequency calculation

Atoms in molecules vibrate relative to each other, including translations (external), rotations (internal), and vibrations. A diatomic molecule has only one motion, while polyatomic N atoms molecules have $3N - 6$ vibrations, known as normal modes. Each has a characteristic mode and frequency. Polyatomic molecules typically vibrate in the following modes: asymmetric, symmetric, wagging, twisting, scissoring, rocking and others.

All calculations, geometry optimizations and frequency calculations and the vibrational frequency calculation, were obtained by the Gaussian 16 suite of programs at the B3LYP/6-31G(d) level of theory. [17] We employed the following four parameters for all normal vibrational modes in this study : Harmonic frequencies ('F', cm $^{**-1}$), reduced masses ('M', AMU), force constants ('C', mDyne/A) and IR intensities ('I', KM/Mole).

2.3 Configuration of CNN_vib

Fig.2 shows the regression with CNN_vib that we carried out in the current study; the explanatory variable is a matrix of four factors (F, M, C and I) for each vibrational mode. We call it 'Calc.Vib.Param.' in this paper. CNN_vib is a multi-output regressor which gives multiple probabilities at once corresponding to each odor descriptor. The output is a matrix of two factors.

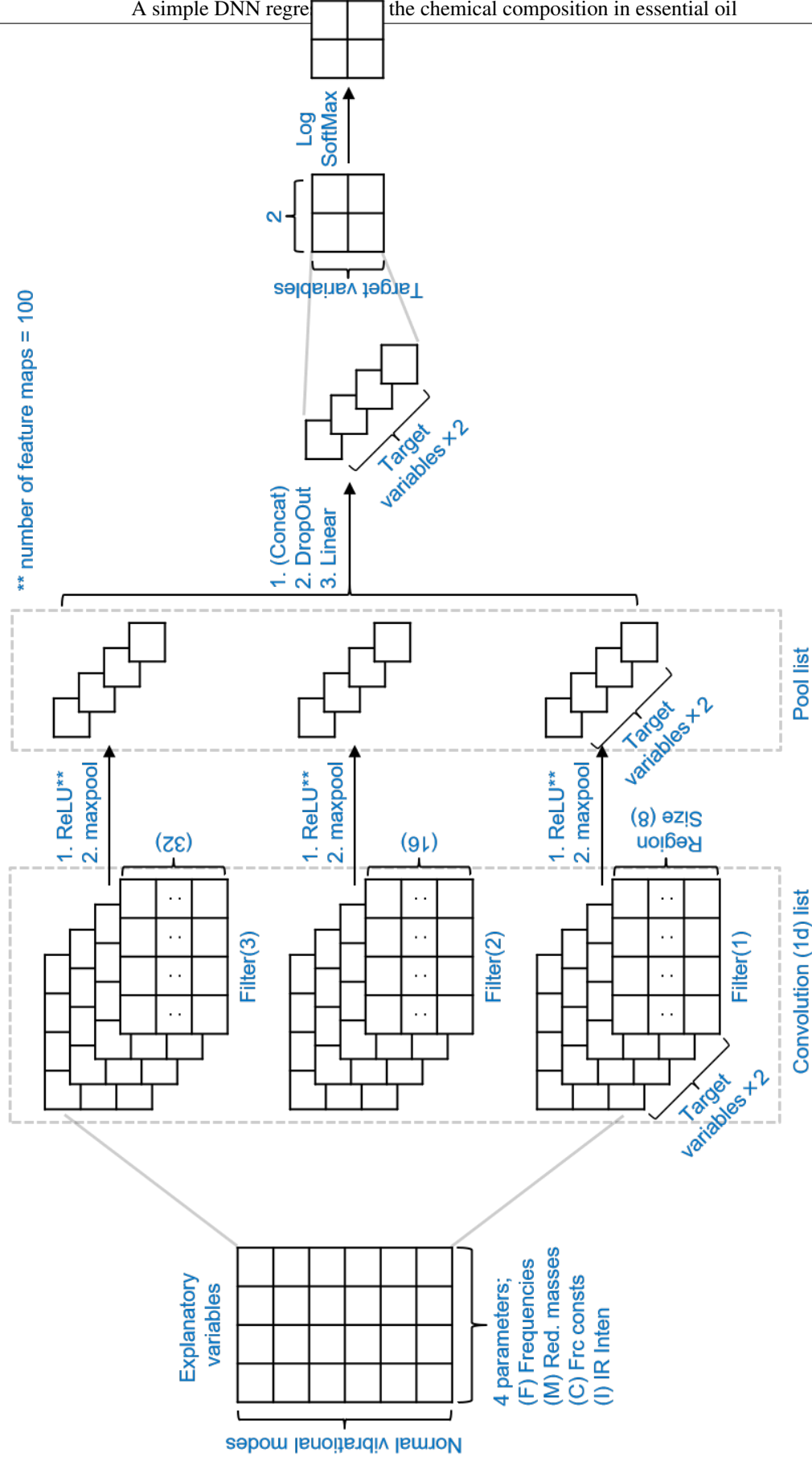


Figure 2: CNN_vib design

The predictability was evaluated using the Area Under the ROC Curve (AUC), which resulted in a value close to one, suggesting high classification accuracy. We utilized k -fold cross-validation to evaluate CNN_vib. Then, the AUCs for each odor descriptor were calculated for training epoch numbers in CNN_vib.

We explored and optimized the design of CNN_vib as well as their hyperparameters. The details of CNN_vib design, such as the selection or sorting of explanatory variable matrix, hyperparameter tuning, the overlearning behavior and reproducibility are described in SI.

2.4 Configuration of the logistic regression based on vibrational spectra

We also performed logistic regression based on vibrational spectra, which gives the probability of an odor descriptor. The spectra were obtained 'F' and 'I' from 'Calc.Vib.Param.' after preprocessing. The preprocessing includes normalizing and 'moving sum', which is creating a series of sum of different selections of the full data set (see details in SI Fig.S003). We call it 'Calc.Spectra' in this paper. The predictability was evaluated using the AUCs for each odor descriptor. AUCs were obtained by iterative k -fold cross-validation of the regression model for each odor descriptor, following the previous report.[12]

2.5 Configuration of logistic regression with FPs

We performed logistic regression with four FPs, including MACCS keys, Extended-Conectivity Fingerprints (ECFPs), Avalon fingerprints, and RD-kit fingerprints (RDKFP), in the previous report. [12] The predictability was evaluated using the AUCs. AUCs were obtained by iterative k -fold cross-validation of the regression model, for each odor descriptor, for each FP.

3 Result and Discussion

We investigated (i) CNN_vib with 'Calc.Vib.Param.', (ii) the logistic regression with 'Calc.Spectra', and (iii) the logistic regression with FPs. The result concerning predictability in the three is summarized in Table 1. It is also visualized in Fig.3. The horizontal axis is the structural diversity, for which we adopted a conventional approach of Tanimoto similarity scores as an index in the current study. The vertical axis is the AUC for each odorants group.

In our previous study, we reported regression analysis and mapping based on the odorant chemical space, based on four conventional FPs: MACCS keys, ECFPs, Avalon fingerprints, and RDKFP. We found that the difficulties relates to the complexity included in the odor descriptor, and that the strong interplay is traced between structural diversity and the predictability of the odor descriptor, by all four FPs; the essential arguments are qualitatively conserved among the four fingerprints. [12].

As a natural extention of previous study, in this study we evaluated differences in predictabilities of each regression from (i) and (ii). As a result, "wood" and "alkane", which had a high AUC in (iii), are also assigned with a high AUC in CNN_vib. In the same way, "must", "medicine" and "sweet", which had a small AUC in (iii), are also assigned with a small AUC in CNN_vib. So far, we confirm the previously reported argument in three regressors. By contrast, we find a new feature obtained by CNN_vib. It is noteworthy that the new feature is possible to be obtained only by CNN_vib to be discussed in 3.1.

3.1 Comparison of predictability in three regressors

At the simple CNN architecture, although we introduced a new algorithms different from logistic regression, the predictability of "wood", "citrus", and "mint" group by CNN_vib is almost the same performance in comparison to that by logistic regression. By contrast, the predictability of "roast", "sulfur", and "cabbage" group by CNN_vib is less than that by logistic regression as shown in Table 1 (see marked with *). It suggests that CNN_vib may offer a qualitatively different perspective. We will discuss the differences in predictability at the CNN_vib depending on odorant group.

Fig.4 shows the examples of molecular structure in these six group. The following trends are observed. In the "wood" group (Fig.4(A)), hydrocarbon-sesquiterpenes are dominant having conventional functional groups such as ethers, alcohols, and ketones. In the "citrus" group (Fig.4(B)), terpenes are dominant which have conventional functional groups such as alcohols and aldehydes. The "mint" group (Fig.4(C)) contains menthol-like skeletons having conventional functional groups such as ketones, and also contains salicylic acid. Although the parent skeletons are diverse with various functional groups, even with the different functional groups, we infer that the similar vibrational modes can occur and give the high AUC by CNN_vib. The "sulfur" group (Fig.4(D)) has distinctive S-containing functional groups. In the "roast" group (Fig.4(E)), pyrazines or thiazoles are dominant. The logistic regression with 'Calc.Spectra' for the

Odor Descriptors (Regr. / Exp. Var.) (Number of Odorants)	Average of Tanimoto Scores				"Conventional FP"				"Vibrational motion"		(Note)	
					Logistic regression (LR)				LR	CNN_vib		
	ECFP	MACCS	Avalon	RDK FP	ECFP	MACCS	Avalon	RDKFP	Calc.Spectra	Calc.Vib.Param.		
fruit	69	0.174	0.413	0.249	0.200	0.755	0.744	0.721	0.718	0.649	0.649	
green	62	0.144	0.348	0.229	0.170	0.733	0.658	0.744	0.707	0.656	0.576	
sweet	60	0.110	0.293	0.169	0.123	0.597	0.565	0.606	0.644	0.596	0.548	
wood	46	0.144	0.529	0.284	0.311	0.899	0.919	0.870	0.893	0.882	0.873	-
herb	45	0.128	0.387	0.212	0.188	0.750	0.774	0.758	0.764	0.670	0.720	
flower	45	0.122	0.311	0.188	0.132	0.745	0.660	0.729	0.713	0.640	0.678	
spice	42	0.118	0.333	0.204	0.183	0.855	0.814	0.864	0.811	0.688	0.698	
fat	35	0.302	0.536	0.339	0.283	0.904	0.863	0.841	0.866	0.778	0.812	
sulfur	22	0.102	0.231	0.178	0.085	0.927	0.942	0.961	0.952	0.923	0.452	-
citrus	22	0.143	0.391	0.233	0.168	0.799	0.783	0.782	0.702	0.704	0.761	-
mint	20	0.143	0.417	0.255	0.219	0.777	0.782	0.811	0.770	0.662	0.775	-
earth	20	0.114	0.320	0.237	0.169	0.740	0.750	0.812	0.772	0.646	0.762	
alkane	20	0.914	0.956	0.911	0.859	1.000	1.000	1.000	1.000	0.996	0.996	
roast	19	0.161	0.331	0.262	0.144	0.902	0.918	0.934	0.892	0.805	0.609	-
must	17	0.113	0.289	0.170	0.108	0.415	0.445	0.502	0.318	0.514	0.527	
oil	16	0.185	0.436	0.225	0.192	0.756	0.724	0.711	0.618	0.784	0.590	
pungent	16	0.217	0.371	0.251	0.215	0.843	0.919	0.908	0.879	0.773	0.432	
balsamic	16	0.117	0.269	0.186	0.141	0.750	0.735	0.817	0.804	0.712	0.544	
rose	15	0.277	0.664	0.392	0.321	0.875	0.938	0.893	0.883	0.806	0.773	
fresh	15	0.141	0.403	0.204	0.181	0.564	0.632	0.565	0.704	0.615	0.602	
apple	14	0.281	0.548	0.437	0.351	0.953	0.892	0.903	0.923	0.858	0.863	
caramel	14	0.176	0.399	0.315	0.170	0.900	0.952	0.937	0.802	0.899	0.728	
wax	13	0.148	0.481	0.282	0.208	0.737	0.826	0.696	0.732	0.863	0.655	
honey	11	0.239	0.368	0.283	0.247	0.905	0.858	0.668	0.613	0.795	0.777	
nut	11	0.142	0.296	0.182	0.134	0.637	0.821	0.716	0.803	0.684	0.582	
metal	10	0.231	0.443	0.275	0.226	0.838	0.611	0.847	0.847	0.595	0.767	
sweat	10	0.248	0.409	0.360	0.330	0.884	0.918	0.963	0.939	0.705	0.543	
camphor	10	0.191	0.555	0.402	0.351	0.950	0.834	0.882	0.889	0.939	0.806	
coconut	10	0.322	0.626	0.385	0.470	0.958	0.939	0.869	0.939	0.837	0.837	
cabbage	10	0.152	0.247	0.225	0.153	1.000	0.979	0.989	1.000	0.984	0.648	-
medicine	10	0.120	0.240	0.192	0.094	0.711	0.737	0.571	0.682	0.579	0.506	
turpentine	9	0.162	0.472	0.257	0.263	0.885	0.903	0.838	0.863	0.837	0.827	
lemon	9	0.163	0.464	0.241	0.249	0.751	0.808	0.827	0.818	0.560	0.652	
rancid	9	0.162	0.265	0.227	0.223	0.897	0.755	0.984	0.895	0.869	0.565	
cucumber	8	0.365	0.625	0.491	0.409	0.958	0.968	0.948	0.895	0.843	0.842	
mushroom	8	0.242	0.463	0.318	0.235	0.900	0.884	0.882	0.804	0.647	0.608	
soap	8	0.370	0.650	0.441	0.346	0.919	0.917	0.985	0.913	0.779	0.854	
(Average AUC)	-	-	-	-	0.821	0.815	0.816	0.805	0.751	0.687		

Table 1: The AUCs by three regressor; (i) CNN_vib with calculated vibrational parameters ('Calc.Vib.Param.'), (ii) the logistic regression based on vibrational spectra ('Calc.Spectra'), and (iii) the logistic regression with four conventional FPs: MACCS keys, ECFPs, Avalon fingerprints, and RDKFP.

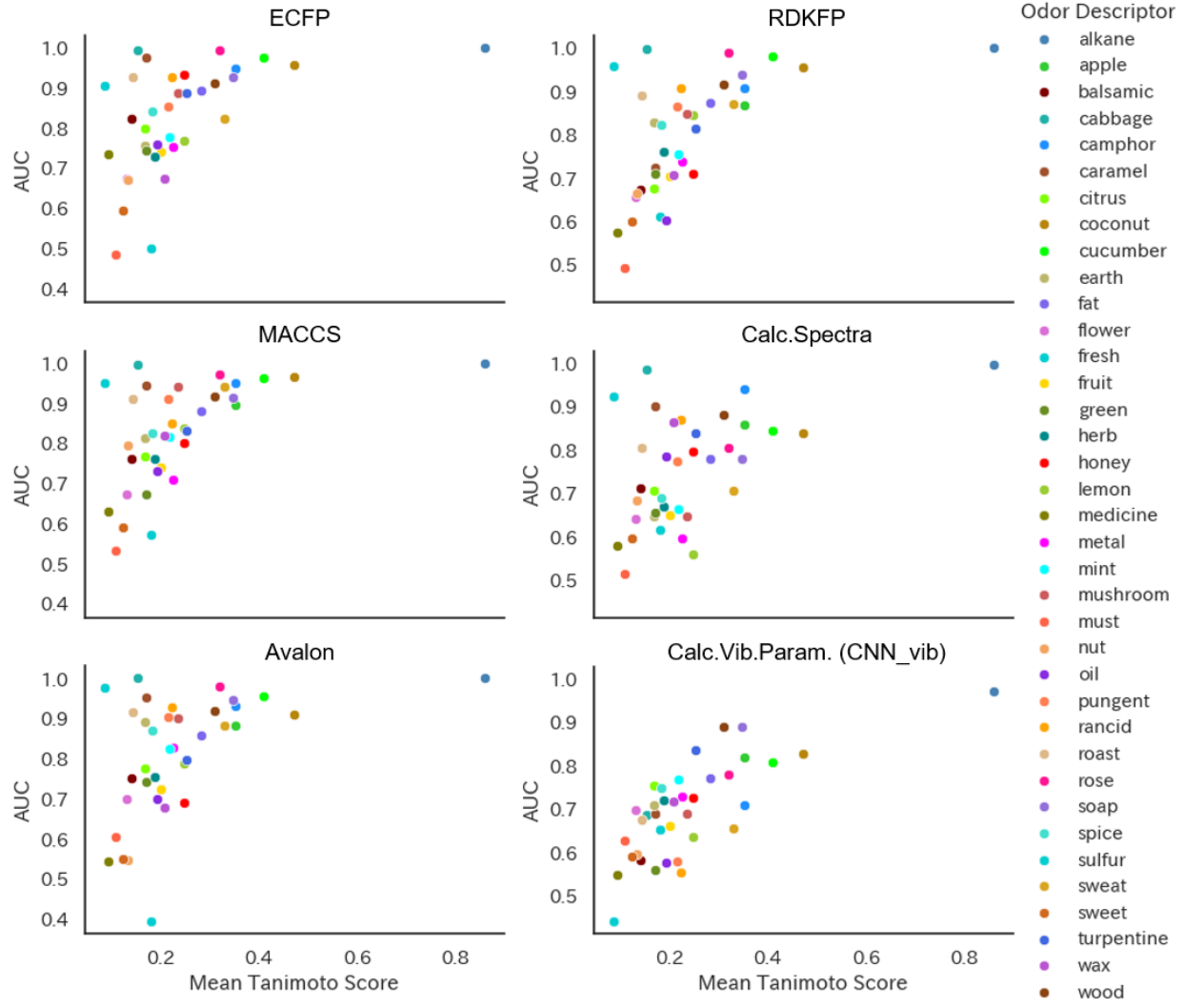


Figure 3: Similarity average vs AUC for each odorants group

"sulfur" and "roast" group show slightly inferior predictability to conventional FPs (see column 'Calc.Spectra' in Table 1).

This indicates that their structural feature may have a superior explanatory ability to the vibrational features for this case. The "cabbage" group (Fig.4(F)) has distinctive thioisocyanates or S-containing groups. Because the parent skeletons are diverse, with the characteristic functional groups on their skelton, the resulting 'Calc.Vib.Param.' vary widely. CNN_vib shows only low predictability, because the vibrational modes are dissimilar (see also in Fig.S008-S013). Their structure are diverse in the "sulfur" group and the "cabbage" group. Notice that high predictability is obtained through the regression with 'Calc.Spectra' processed with moving sum. Such a softening of vibrational characteristics is expected to produce good predictability.

3.2 Which descriptors demonstrated regression performance with molecular vibrations ?

In the group "wood", "citrus" and "mint", because of their similar molecular structures as shown in Fig.4. it is potentially difficult that these molecules can be sniffed out in olfactory cognition. As a matter of fact, human will be able to distinguish their odor characteristics through repeated training. Then, it is a difficult question whether we can sniff out without training or not. It means that our culture has fine-resolitional cognition with using fine-resolitional *evaluation word*, despite the strongly biased diversity for the three groups.

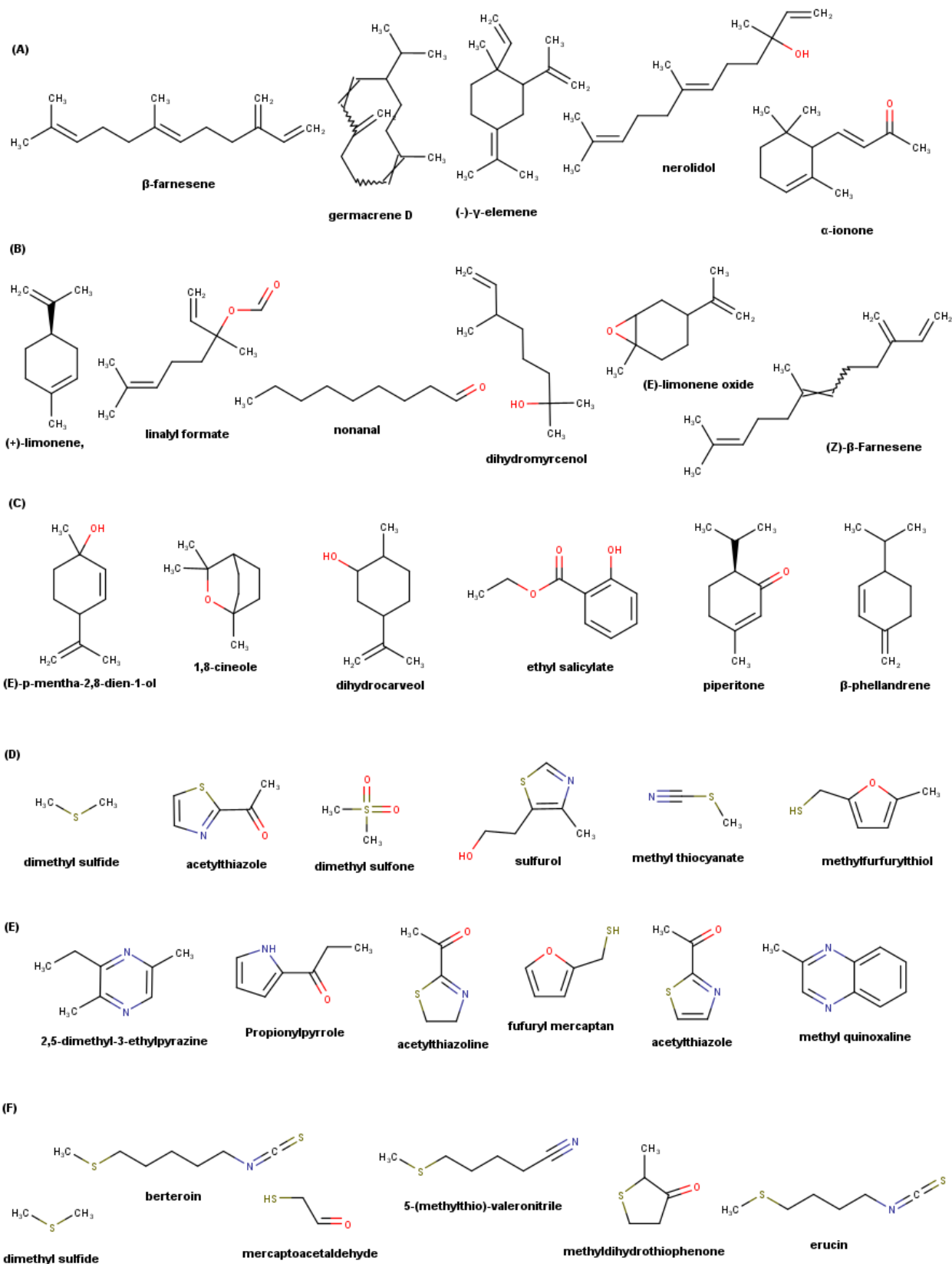


Figure 4: Example molecules in (A)"wood", (B)"citrus", (C)"mint", (D)"sulfur", (E)"roast", and (F)"cabbage" group

On the other hands, the "roast", "sulfur" and "cabagge" groups have distinctive functional groups and can be smelled at a low threshold. Thus, they can be sniffed out in olfactory cognition and clearly apply these *evaluation word*, leading to strong structure-odor relationship. Because of their structural diversity except their distinctive functional groups, CNN_vib has only modest predictability for these groups. We had better consider the possibility that both cognitional and linguistic biased resolutional distributions must be taken into account in this regression study. This will be a very challenging subject in future for chemistry, data science and also for cognitive study.

3.3 Insights into *theory of olfaction* beyond molecular substructure

We attempted to investigate whether the molecular vibration is truly irrelevant to their odor descriptors with two regressors; logistic regression and CNN_vib. The *shape theory of olfaction*, widely accepted concept of the olfaction, means that odorant molecules are recognized by their shapes, much like a key fits into a lock of olfactory receptor. Because these four FPs comprise of molecular substructures in a ligand molecule, they closely match the interaction and recognition of the *shape theory of olfaction*. Our study demonstrated that 'Calc.Spectra' with logistic regression shows predictability, and that 'Calc.Vib.Param.' with CNN_vib also shows predictability. We found that the molecular vibration has explanatory ability on odorant characters, rather than their shapes alone (not irresponsible for olfaction).

3.4 Insights into chemical space representation

Some researches, inspired by the development of neural networks, in recent years have been published; image classification and segmentation, applications of Natural language Processing for line notations [18] and graph neural network (GNN) model. [19, 20, 21, 22, 23] Some regression studies indicated that the line notations model and graph neural networks performed even worse than image recognition-based models, [18] although their machine learning architectures are well-suited to chemical compounds. Even if their prediction performance has not yet meet expectations, those models have much rooms to be studied more profoundly.

CNN_vib can read data in a variety of shapes and showed predictability: the explanatory variables, derived from vibrational frequency calculations, change shape according to their vibrational modes that correspond to the molecular complexity. It offers a fascinating alternative or complementary perspective, when the viewpoint shifts from static/spatial to motional or dynamic/temporal for the chemical space representation. In contrast, since the explanatory variable in conventional machine learning regression should have the same size of structure, reshaping of the parameters to spectrum is unavoidable for logistic regression. When investigating chemical space exploration with complex input or by nonlinear model, further deep learning techniques are to be studied. Our CNN_vib demonstrated some explanatory ability of deep learning techniques on this problem. Such a techniques has the potential to improve the chemical space representation beyond molecular substructure and forecast physical attributes.

4 Conclusions

In this study, we investigated (i) the CNN with molecular vibrational parameters ('Calc.Vib.Param.'), (ii) the logistic regression based on vibrational spectra ('Calc.Spectra'), and (iii) the logistic regression with four conventional FP. Our investigation demonstrates that both (i) and (ii) provide predictability and that (i), (ii) and (iii) show nearly the same tendencies in their predictability. It was also found that the predictabilities for some odor descriptors of (i) and (ii) are comparable to those of (iii). If the parent skeletons are diverse with the characteristic functional groups on their skeletons, their structural feature may have explanatory ability than the vibrational features, thus vibrational feature may not show predictability, because the resulting vibrational mode parameters vary widely. Our research demonstrated that the molecular vibration has explanatory ability on odorant characters. To improve the chemical space representation capable of predicting physical properties, our findings provide insight into the representation of molecular features beyond molecular substructure.

5 Data and Software Availability

We used the RDkit [7] for the FPs (MACCS, ECFPs, Avalon fingerprint and RDKitFP) . The regression methodology, multi variate analysis and mapping is proprietary but not restricted to our program. The following Supporting Information is available; SourceAndSummary.zip (source and summary tables of regression results), out_files.zip (Gaussian 16 output files for the odorants) and input_files.zip (Gaussian 16 input files for the odorants).

Table 2: List of abbreviations

Abbreviations	Description
'F'	Harmonic Frequencies (cm**-1)
'M'	Reduced Masses (AMU)
'C'	Force Constants (mDyne/A)
'T'	IR Intensities (KM/Mole)
ECFPs	Extended-Conectivity Fingerprints
RDKFP	RD-kit Fingerprints
IR	Infrared (Spectra)
GCO	Gas Chromatography Olfactometry
FP(s)	Fingerprint(s)
AUC	Area Under the (ROC) Curve
DNN	Deep Neural Network
CNN	Convolutional Neural Network
GNN	Graph Neural Network

6 List of abbreviations

7 Acknowledgments

The authors thank the anonymous reviewers for their valuable suggestions. This work was supported by Shorai Foundation for Science and Technology. The source code and related materials are available at our GitHub repository. [24]

References

- [1] Jean-Louis Reymond. The chemical space project. *Accounts of Chemical Research*, 48(3):722–730, 2015.
- [2] Dmitry I Osolodkin, Eugene V Radchenko, Alexey A Orlov, Andrey E Voronkov, Vladimir A Palyulin, and Nikolay S Zefirov. Progress in visual representations of chemical space. *Expert opinion on drug discovery*, 10(9):959–973, 2015.
- [3] Emily J Mayhew, Charles J Arayata, Richard C Gerkin, Brian K Lee, Jonathan M Magill, Lindsey L Snyder, Kelsie A Little, Chung Wen Yu, and Joel D Mainland. Drawing the borders of olfactory space. *bioRxiv*, pages 2020–12, 2020.
- [4] Emily J Mayhew, Charles J Arayata, Richard C Gerkin, Brian K Lee, Jonathan M Magill, Lindsey L Snyder, Kelsie A Little, Chung Wen Yu, and Joel D Mainland. Transport features predict if a molecule is odorous. *Proceedings of the National Academy of Sciences*, 119(15):e2116576119, 2022.
- [5] Jason B Castro, Travis J Gould, Robert Pellegrino, Zhiwei Liang, Liyah A Coleman, Famesh Patel, Derek S Wallace, Tanushri Bhatnagar, Joel D Mainland, and Richard C Gerkin. Pyrfume: A window to the world’s olfactory data. *bioRxiv*, pages 2022–09, 2022.
- [6] Alice Capecchi, Daniel Probst, and Jean-Louis Reymond. One molecular fingerprint to rule them all: drugs, biomolecules, and the metabolome. *Journal of cheminformatics*, 12:1–15, 2020.
- [7] RDKit: Open-source cheminformatics. <https://www.rdkit.org>.
- [8] Davide Boldini, Davide Ballabio, Viviana Consonni, Roberto Todeschini, Francesca Grisoni, and Stephan A Sieber. Effectiveness of molecular fingerprints for exploring the chemical space of natural products. *Journal of Cheminformatics*, 16(1):35, 2024.
- [9] Bruno J Neves, Rodolpho C Braga, Cleber C Melo-Filho, José Teófilo Moreira-Filho, Eugene N Muratov, and Carolina Horta Andrade. Qsar-based virtual screening: advances and applications in drug discovery. *Frontiers in pharmacology*, 9:1275, 2018.
- [10] M Chastrette. Trends in structure-odor relationship. *SAR and QSAR in Environmental Research*, 6(3-4):215–254, 1997.
- [11] Benjamin Sanchez-Lengeling, Jennifer N Wei, Brian K Lee, Richard C Gerkin, Alán Aspuru-Guzik, and Alexander B Wiltschko. Machine learning for scent: Learning generalizable perceptual representations of small molecules. *arXiv preprint arXiv:1910.10685*, 2019.

- [12] Yuki Harada, Shuichi Maeda, Junwei Shen, Taku Misonou, Hirokazu Hori, and Shinichiro Nakamura. Regression study of odorant chemical space, molecular structural diversity, and natural language description. *ACS omega*, 2024.
- [13] Luca Turin. A spectroscopic mechanism for primary olfactory reception. *Chemical senses*, 21(6):773–791, 1996.
- [14] Eric Block, Seogjoo Jang, Hiroaki Matsunami, Sivakumar Sekharan, Bérénice Dethier, Mehmed Z Ertem, Sivaji Gundala, Yi Pan, Shengju Li, Zhen Li, et al. Implausibility of the vibrational theory of olfaction. *Proceedings of the National Academy of Sciences*, 112(21):E2766–E2774, 2015.
- [15] Leslie B Vosshall. Laying a controversial smell theory to rest. *Proceedings of the National Academy of Sciences*, 112(21):6525–6526, 2015.
- [16] T Acree and H Arn. Flavornet home page, 2003.
- [17] MJ Frisch. Gaussian 09 revision d. 01; b) mj frisch, gw trucks, hb schlegel, ge scuseria, ma robb, jr cheeseman, g. scalmani, v. barone, ga petersson, h. nakatsuji et al. *Gaussian 16 Revision A*, 3, 2016.
- [18] Anju Sharma, Rajnish Kumar, Shabnam Ranjta, and Pritish Kumar Varadwaj. Smiles to smell: decoding the structure–odor relationship of chemical compounds using the deep neural network approach. *Journal of Chemical Information and Modeling*, 61(2):676–688, 2021.
- [19] Ziwei Zhang, Peng Cui, and Wenwu Zhu. Deep learning on graphs: A survey. corr abs/1812.04202 (2018). *arXiv preprint arXiv:1812.04202*, 2018.
- [20] Brian K Lee, Emily E Mayhew, Benjamin Sanchez-Lengeling, Jennifer N Wei, Wesley W Qian, Kelsie Little, Matthew Andres, Britney B Nguyen, Theresa Moloy, Jane K Parker, et al. A principal odor map unifies diverse tasks in human olfactory perception. *bioRxiv*, 2022.
- [21] Wesley W Qian, Jennifer N Wei, Benjamin Sanchez-Lengeling, Brian K Lee, Yunan Luo, Marnix Vlot, Koen Dechering, Jian Peng, Richard C Gerkin, and Alexander B Wiltschko. Metabolic activity organizes olfactory representations. *Elife*, 12:e82502, 2023.
- [22] Bohayra Mortazavi. Recent advances in machine learning-assisted multiscale design of energy materials. *Advanced Energy Materials*, page 2403876, 2024.
- [23] Ryan Jacobs, Dane Morgan, Siamak Attarian, Jun Meng, Chen Shen, Zhenghao Wu, Clare Yijia Xie, Julia H Yang, Nongnuch Artrith, Ben Blaiszik, et al. A practical guide to machine learning interatomic potentials–status and future. *Current Opinion in Solid State and Materials Science*, 35:101214, 2025.
- [24] yhua0917@github.com. Motional representation by cnnvib. <https://github.com/yhua0917/MotionalRepresentationByCnnVib>, 2025.